Geophysical Research Letters

RESEARCH LETTER
10.1029/2022GL100735

Silent Very Long Period Seismic Events (VLPs) at Stromboli Volcano, Italy

Kathleen F. McKee[1,2], Diana C. Roman[1], Gregory P. Waite[3], and David Fee[4]

[1]Earth and Planets Laboratory, Carnegie Institution for Science, Washington, DC, USA, [2]Now at NASA Goddard Space Flight Center, Greenbelt, MD, USA, [3]Department of Geological and Mining Engineering and Sciences, Michigan Technological University, Houghton, MI, USA, [4]Wilson Alaska Technical Center, Alaska Volcano Observatory, Geophysical Institute, University of Alaska Fairbanks, Fairbanks, AK, USA

Key Points:

- Seismo-acoustic observations from Stromboli in 2018 show hundreds of repeating very long period (VLP) seismic signals without corresponding acoustic signals
- VLPs without explosions suggest the slug model is a poor fit for "normal" activity at Stromboli
- We suggest VLPs may instead result from large gas bubbles interacting with a semi-permeable solid plug

Supporting Information:

Supporting Information may be found in the online version of this article.

Correspondence to:

K. F. McKee,
kfmckee@alaska.edu

Citation:

McKee, K. F., Roman, D. C., Waite, G. P., & Fee, D. (2022). Silent very long period seismic events (VLPs) at Stromboli Volcano, Italy. *Geophysical Research Letters*, *49*, e2022GL100735. https://doi.org/10.1029/2022GL100735

Received 4 AUG 2022
Accepted 13 NOV 2022

Author Contributions:

Conceptualization: Kathleen F. McKee
Formal analysis: Kathleen F. McKee, Diana C. Roman, Gregory P. Waite
Funding acquisition: Kathleen F. McKee
Investigation: Kathleen F. McKee, Diana C. Roman, Gregory P. Waite, David Fee
Project Administration: Kathleen F. McKee
Resources: Diana C. Roman, David Fee
Visualization: Kathleen F. McKee
Writing – original draft: Kathleen F. McKee, Diana C. Roman, Gregory P. Waite, David Fee
Writing – review & editing: Kathleen F. McKee, Diana C. Roman, Gregory P. Waite, David Fee

Abstract At Stromboli Volcano, Italy, very long period (VLP) seismic signals and Strombolian eruptions have been attributed to the unsteady flow of gas slugs through the shallow plumbing system followed by explosive slug bursting at a free surface. In data from a 2018 seismo-acoustic deployment, ~92% of events in two main VLP multiplets do not coincide in time with impulsive infrasonic signals (the expected signal of explosive slug bursting); we term these "silent VLPs." The lack of infrasonically detected explosions relative to repeating VLPs does not support the commonly invoked "gas slug" model. We propose that VLPs may be generated when gas bubbles move into a weak semi-solid plug in the uppermost portion of the conduit. The plug then acts as a mechanical filter in which pathways vary and guide or trap ascending gas slugs, allowing for passive (silent) gas release and explosive escape mechanisms decoupled in time from VLPs.

Plain Language Summary Very long period (VLP) seismic signals are thought to be produced by magma and gas flow through shallow volcano conduits. At Stromboli Volcano, Italy (the type volcano for Strombolian explosions) and other basaltic volcanoes worldwide, VLPs have been modeled as the result of flow of a gas slug through the conduit followed by an explosion when the slug bursts at a free surface. However, these interpretations do not account for variable crystal content (i.e., systems with three phases: solid, liquid, and gas). Here we show that the standard "slug" model does not hold during a period of intense study at Stromboli in 2018. We compare the timing and characteristics between two repeating VLP families and explosions at the surface, as characterized by acoustic data. The vast majority of VLPs do not have coincident explosions—we term these "silent VLPs." Our observations instead support a "plug" model. We argue that VLPs are generated when gas slugs interact with and move into a weak plug in the uppermost portion of the conduit, which acts as a mechanical filter for gas transport. This interpretation allows for both passive (silent) and explosive gas escape decoupled in time from VLPs.

1. Introduction

Persistent, low-level (VEI 1-2) Strombolian eruptive activity is typical at many open-vent volcanoes around the world. Named after Stromboli (Italy), where the visually spectacular eruptions draw tourists and scientists to observe them from the relative safety of the summit, Strombolian eruptions have long been attributed to a process of gas slug ascent and bursting at a free (liquid) surface based on direct visual observations of bubble bursting at a lava lake at Heimaey Volcano, Iceland, in the 1970s (Blackburn et al., 1976). Strombolian eruptions are also linked to a type of very long period (2–100 s, VLP) seismic signal and the connection to the slug-bursting model has formed the basis for decades of detailed analysis and interpretation of VLPs at volcanoes worldwide, including Stromboli (Chouet et al., 1999; Neuberg et al., 1994); Kilauea, USA (Ohminato et al., 1998); and Erebus, Antarctica (Aster et al., 2008; Knox et al., 2018; Rowe et al., 1998).

The established conceptual model for VLPs links them to the driving mechanism for Strombolian explosions through the acceleration of magma in the conduit around a rising gas slug and/or top-down pressure change caused by the burst of the slug and mass ejection at the surface (Chouet et al., 2003; James et al., 2006). This model predicts an impulsive infrasonic event, or explosion, resulting from the eruption due to the rapid expansion of gases following slug bursting (Bodurtha, 1980; Kinney & Graham, 1985).

We conducted an intensive week-long multi-instrumental field study at Stromboli in May 2018 to investigate the explosive mechanism, which resulted in a detailed catalog of hundreds of VLP events. Instead of clear explosions

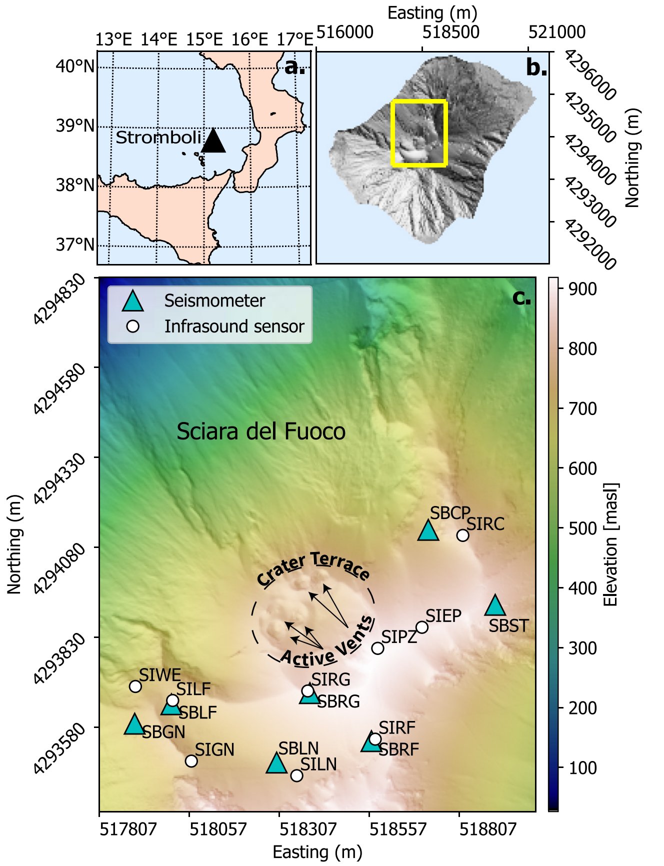

Figure 1. Map of study area. (a) Stromboli is one of the Aeolian Islands north of Sicily, Italy. (b) The Island of Stromboli, and the yellow box is the area shown in (c). (c) Stromboli summit area, with light blue triangles marking the seismometer locations and white circles the infrasound sensors. The black arrows point to active vents.

in the infrasound data, we find an absence of infrasonic signals associated with most VLPs, which conflicts with the "slug" model. We propose a new model for VLPs, first presented by McKee et al. (2019), based on an upper conduit crystal mush "plug" (Oppenheimer et al., 2020; Suckale et al., 2016) that is consistent with our observations. Our proposed model for VLP generation likely applies to other subduction zone volcanoes with high water content basalts that drive significant shallow degassing-induced crystallization, such as Yasur, Vanuatu, and Fuego, Guatemala.

1.1. Stromboli Volcano, Italy

The Strombolian eruptive style is defined by relatively weak, discrete explosions, which eject gas, molten magma, and lithics (Taddeucci et al., 2015), with Stromboli Volcano being the type locale. At Stromboli, the activity is centralized at a crater terrace (Figure 1), which at any given time has 3–10 (or more) active vents aligned from NE to SW (Harris & Ripepe, 2007). Eruptive activity varies from vent to vent and includes: small, ash-rich explosions that eject crystal-rich scoria; gas-rich explosions; gas-jetting events; and constant passive degassing (Ripepe et al., 2008). Jetting is a momentum-driven, fluid flow through a nozzle or vent (Tam, 1998). When a jet flow perturbs the atmosphere it creates a velocity shear causing turbulence which generates sound (Kundu & Cohen, 2008). During this archetypal, long-term average eruptive activity, which we refer to as normal activity, the visually documented explosion rate is about 3–12 explosions per hour (Ripepe et al., 2007) with passive degassing simultaneously occurring from multiple vents. At other times, gravity-driven transitions to effusive activity produce lava flows in the Sciara del Fuoco (Figure 1) (Falsaperla et al., 2008; Marsella et al., 2012). During effusive activity, the number and amplitude of VLPs remains high, but their relative source location is deeper in the magmatic conduit (Ripepe et al., 2015).

1.2. Models for Activity at Stromboli

There are currently two primary models for normal shallow eruptive processes at Stromboli Volcano: slug (Blackburn et al., 1976) and plug (Suckale et al., 2016). The models are likely applicable to other volcanoes around the world characterized by Strombolian activity. Here we describe the two conceptual models and later we evaluate the conceptual models in light of our seismo-acoustic observations.

1.2.1. Slug Model

The slug model was based on visual observations of explosions at (a) Heimaey Volcano in February 1973, where the eruption started as a 1,500 m long fissure eruption (Thorarinsson et al., 1973) and evolved to steady lava effusion through three vents at the time of observation, and (b) Stromboli Volcano in April 1975 (Blackburn et al., 1976). Blackburn et al. (1976) note there was significantly greater mass of gas erupted than solid particles in both systems, and the amount of gas erupted required a larger volume of magma than was erupted. They suggested that Strombolian explosions thus represent the bursting of large bubbles at a magma free surface, and that the pyroclasts are magma fragmented by the bubble expansion. The slug model is simple, explains the high gas/magma output of Strombolian explosions, and is consistent with observations at systems such as Kilauea (Chouet et al., 2010; Ohminato et al., 1998) or Erebus (Knox et al., 2018) where bursting bubbles have been observed at the surface of lava lakes. However, the slug model considers only a two-phase (melt/gas) magma, while magma commonly contains crystals (Francalanci et al., 2004, 2005; Métrich et al., 2001), and it assumes no difference in bubble bursting processes between an open lava lake and a closed to partially open system. Early observations of VLPs at Stromboli were linked to the slug model (Chouet et al., 2003) despite the lack of an observable free surface and the lack of an independent and complete chronology of explosions. Previous work suggests that these large bubbles interact with the conduit walls and generate a VLP as they pass a bend or flare and then explode at the surface (Chouet et al., 2003; James et al., 2006).

1.2.2. Plug Model

Recently an alternate to the slug model was proposed based on 1-D modeling of gas flow through a crystal mush (Suckale et al., 2016). The model of Suckale et al. (2016) involves a semi-permeable solid plug in the top several hundred meters of the conduit of Stromboli volcano that modulates gas escape processes. In this model, gases percolate through this plug continually heating the pathways through which they travel. Pathways with high gas flux and thus high heat flux remain hot and therefore less restrictive gas escape routes (passive degassing). Pathways with lower gas flux are less hot, open due to tensile failure, and ultimately lead to explosive gas escape (explosions and jetting) (Suckale et al., 2016). In support of their conceptual model they note several observations: (a) the top few 100 m of Stromboli's magma column contains highly porphyritic, water-poor magma with 45%–60% phenocrysts and microphenocrysts, which erupt as scoria (Francalanci et al., 2004, 2005; Métrich et al., 2001); (b) low-porphyritic, water-rich magma with <10 vol% phenocrysts originates at approximately 3 km depth and erupts as pumice during major eruptions (Bertagnini et al., 2003; Francalanci et al., 2004, 2005; Métrich et al., 2001); (c) rapid crystallization of plagioclase occurs at around 10 MPa (400–600 m depth) (Agostini et al., 2013; Conte et al., 2006); (d) the crater terrace, crater, and vent locations have been stable for hundreds of years and accommodate both continuous degassing and normal explosions (Calvari et al., 2005; Ripepe et al., 2005); (e) a common gas source feeds the vents several hundred meters below the surface (Genco & Ripepe, 2010; Kirchdörfer, 1999; Wielandt & Forbriger, 1999); and (f) self-potential surveys suggest there is a convective cell of gas and dense magmatic liquid (Ballestracci, 1982; Finizola et al., 2003). However, we note the crater/vent location stability and common gas source are also consistent with the slug model. While rapid crystallization at 10 MPa is noted, the 1-D modeling shows the plug thickness varies from several meters to about 800 m (Suckale et al., 2016). Ultimately the "plug" model considers the crystal-rich nature of the magma erupted at Stromboli. However, it does not address observations of varying gas signature between explosions and passive degassing (Aiuppa et al., 2010) or consider effects from the latent enthalpy of crystallization (Blundy et al., 2006).

2. Field Experiment

We deployed seven seismometers and infrasonic microphones between 12 and 19 May 2018 at the summit of Stromboli (Figure 1, McKee et al., 2018). We sampled the seismic wavefield at 100 Hz. The seismic stations consisted of Nanometrics Trillium 120 Compact Posthole sensors with Centaur digitizers. We deployed seven campaign Chaparral Physics Model 60 UHP infrasonic microphones with DiGOS DATA-CUBE digitizers and sampled the acoustic wavefield at 400 Hz. The average distance from vent to infrasonic sensor is 475 m.

3. Seismo-Acoustic Observations

Eruptive activity during the field campaign was characterized by fewer explosions (less than 2/hr by acoustic detection) with lower energy than normal activity, jetting from a small vent in the southwestern crater, and passive degassing from an incandescent central vent. Using a coincident recursive short-time-average/long-time-average (STA/LTA) trigger, we detected 1,900+ seismic events over the 7 days experiment period. We used a short- and long-term window duration of 10 and 20 s, respectively, and required that 4 of the 7 stations have an STA/LTA ratio above 1.3. These seismic events were generally broadband with energy from 0.01 to 10 Hz. Most had VLP energy in the 0.01–0.5 Hz band (2–100 s period). A small number of events had little to no energy below 1 Hz. We focus subsequent analyses on the VLP component of these broadband seismic events.

We detected ~200 explosions (defined as discrete infrasonic events) using the same STA/LTA trigger and window lengths, and required 4 out of 7 stations to trigger with a ratio of 1.4. The explosions are broadband with energy from 0.1 to >20 Hz and peak pressures ranging from 2 to 72 Pa at about 500 m from the vent (Figures S2a and S2b in Supporting Information S1). We also identified about 500 jetting events, which span the infrasound and audible bands with energy up to at least 100 Hz, and have an impulsive onset and cessation. Jetting events were clearly audible to observers on the summit.

10.1029/2022GL100735

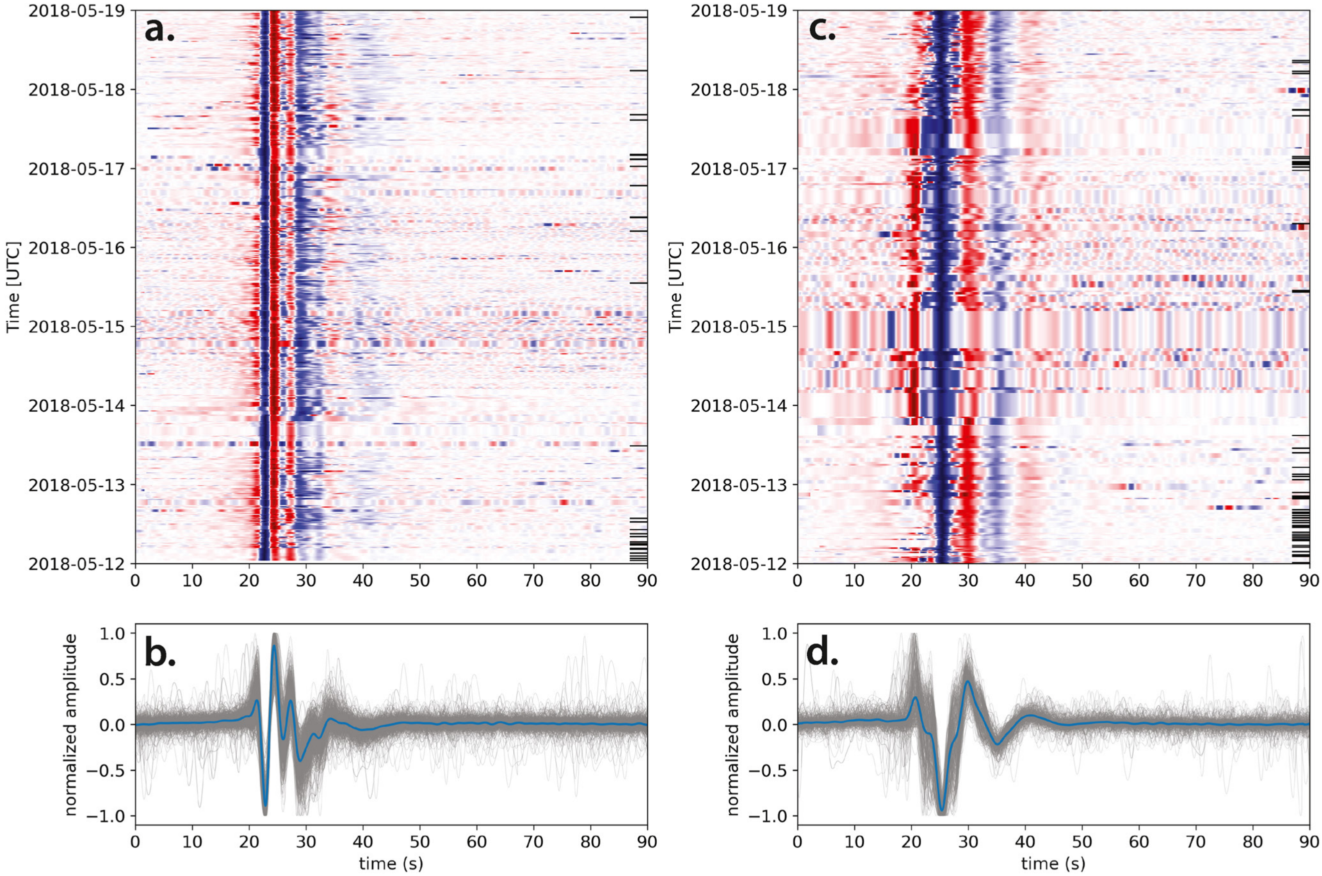

Figure 2. Waveforms from seismic station SBCP for Families 1 and 2. (a) Shows time-aligned (*x*-axis) vertical component waveforms of Family 1 (F1) very long period (VLPs) plotted through time (*y*-axis). The F1 VLP repeats 500+ times over 7 days. Red is positive amplitude or upward motion of the ground and blue is negative or downward motion. For (b), the onset time-aligned VLPs are plotted on top of each other in gray and their average in blue. Similar plots for Family 2 are shown in (c and d), which occurs about 200 times over the same period. In (a) and (c) when the VLP signal appears stretched or blurred vertically it indicates extended time between VLPs, sometimes on the order of hours. The black horizontal ticks on the right *y*-axis of (a) and (c) indicate that the VLP happened at the same time as an explosion at the surface as recorded with infrasound sensors. Waveform amplitudes are normalized.

4. Seismic Multiplet Analysis and VLP Characterization

We used PeakMatch to conduct multiplet analysis of all VLP events (Rodgers et al., 2015). Prior to cross-correlation, we removed the instrument response from the VLP waveforms and filtered events from 0.01 to 0.5 Hz (2–100 s). We windowed event waveforms starting 20 s prior to and 70 s after event onset. We executed PeakMatch such that all unique pairs of waveforms are fully cross-correlated. To assign a VLP to a given multiplet, we required its correlation value to be 0.7 or higher. Full details of the method are described by Rodgers et al. (2015).

The majority (68%) of detected VLPs comprise two main families with more than 100 events that span the 7 days of observation, along with 8 smaller families with 5–70 events in each. We focus subsequent analysis on the main two: Family 1 (F1) and Family 2 (F2). Figure 2 shows F1 and F2 VLPs through time and their respective stack recorded at seismic station SBCP. The horizontal black bars on the right side of Figures 2a and 2c indicate when an impulsive, infrasonic signal began within 10 s of the start of the VLP. F1 has over 500 events, each lasting approximately 25–30 s (Figures 2a and 2b). F2 has over 100 events and they are slightly longer in duration (25–35 s) (Figures 2c and 2d). F1 VLPs have a peak frequency of about 0.2 Hz (5 s), while F2 VLPs' peak frequency is about 0.1 Hz (10 s). Both VLPs are part of a broadband seismic signal (Figures S1, S2c, and S2d in Supporting Information S1). The waveforms for each family are similar in period, shape, and duration from station to station (Figure S3 in Supporting Information S1) and pervasive throughout the week-long study period.

We find that most VLPs are not associated with detected explosions or jetting events (Figure 3a). Figures 3a and 3b show the VLP peak amplitude through time and infrasonic trace peak amplitude through time, respectively.

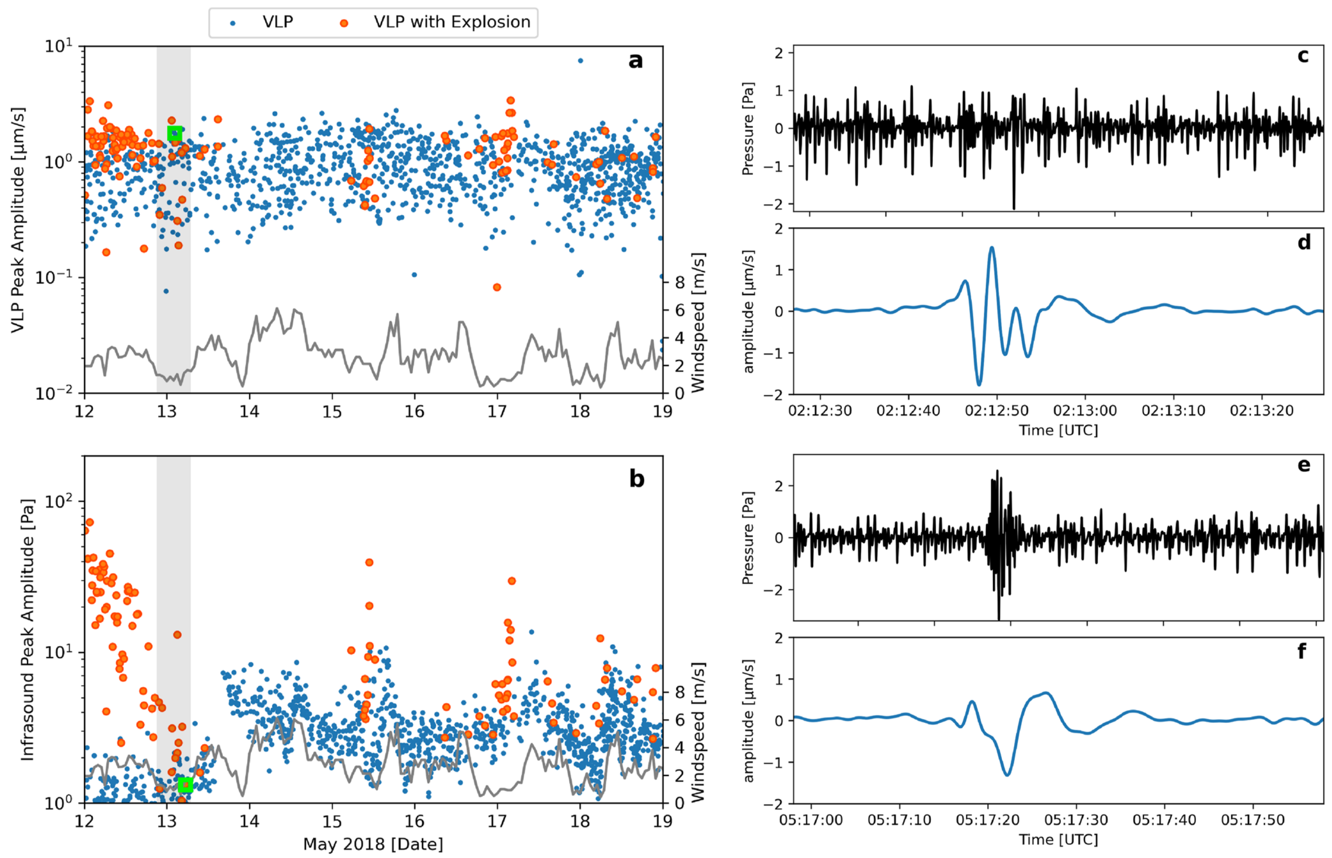

Figure 3. Very long period seismic event (VLP) peak amplitude from station SBCP (a) through time and (b) infrasound peak amplitude through time in the window 10 s prior to 20 s after the VLP onset. VLPs and infrasound amplitudes with an associated explosion signal detected in the infrasound data are in orange, and silent VLPs are in blue. The gray line is the wind speed recorded at a weather station about 72 km to the SSE in Messina, Italy. In (c–f), we show examples of two VLPs recorded during a period of low infrasonic background noise (gray line and gray vertical bars in (a–b). (c–d) show an example of a high-amplitude "silent VLP" (green dot in a) with no corresponding infrasonic signal of explosion, and (e–f) show an example of a VLP with a corresponding low-amplitude infrasonic signal of explosion (green dot in b). (c) Infrasound trace from station SIEP band-pass filtered at 0.5–10 Hz (d) F1 VLP seismic trace from station SBCP filtered between 2–100 s. (e) same as (c) and (f) same as (d) but for a Family 2 (F2) VLP.

Associated, detected explosions are highlighted in orange. This highlights the low rate of explosions relative to VLPs and the poor correlation between infrasonic and VLP peak amplitudes regardless of a detected explosion. About 4% and 1.6% of F1 VLPs align in time with explosions and jetting events, respectively, and about 28% and 4% of F2 VLPs align in time with explosions and jetting events, respectively. Figures 3c and 3d show an example of a Family 1 VLP and the corresponding infrasound data where there is neither an explosion or jetting event. Figures 3e and 3f show an example of an F2 VLP and the corresponding infrasound data in which there is an explosion. Note for Figure 3, the traces have not been shifted to account for travel time. Travel time for the infrasound ranges from 0.7 to 2.3 s depending on the station with an assumed air temperature of 25°C and sound speed c = 346 m/s. Travel time for the seismic *P*-wave ranges from 0.12 to 0.24 s with an assumed velocity of 3,500 m/s (Chouet et al., 2003).

Although we have shown evidence that silent VLPs do occur at Stromboli, we concede that some of the silent VLPs in our catalog that occurred during periods of higher infrasonic noise may in fact have smaller explosion signals. Future work is needed to determine the exact percentage of silent versus non-silent VLPs. The study should be based on a longer period of observation with co-deployed wind sensors to assess silent VLP occurrence over longer periods of low/no background noise than possible given the short duration of our deployment.

For the VLPs that have corresponding explosions, infrasound onset aligns with the higher frequency seismic wave arrival, and the VLP signal starts earlier (Figures 3e and 3f and Figure S2 in Supporting Information S1). Figure 4 shows the particle motion for an F1 and F2 event. The particle motions and source locations are similar

10.1029/2022GL100735

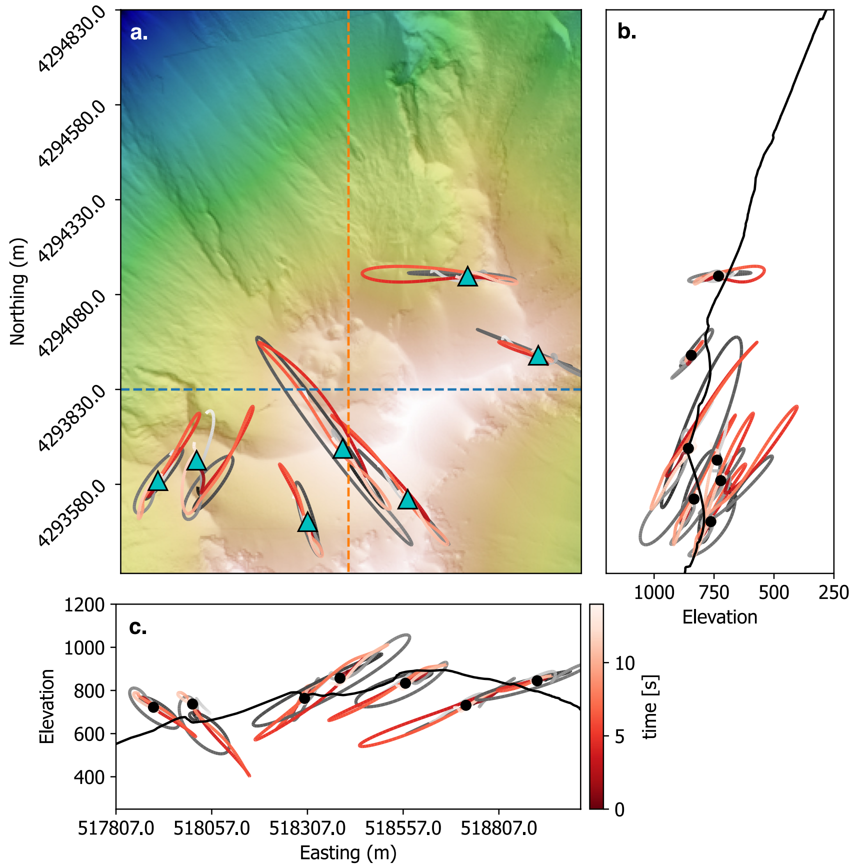

Figure 4. Particle motion for a Family 1 (F1) and Family 2 (F2) very long period event. Further details of each in Figures S1 and S2 in Supporting Information S1. (a) Map view of particle motions with seismometer locations marked by light blue triangles. F1 event is plotted in gray and F2 in red. (b) North versus vertical and (c) East versus vertical particle motion.

between the two events. We examined the particle motion dip for all the VLPs in our catalog including those in F1 and F2. The dip of the VLP particle motion is $-7.2 \pm 2.9°$ for F1 and $-8.2 \pm 2.5°$ for F2 at station SBST, which corresponds to a depth of 140 ± 30 m and 150 ± 25 m vertically below the center of the crater, respectively (Figure S4 in Supporting Information S1).

5. "Silent" VLPs

Our analysis indicates that during a period of relatively low activity VLPs are consistently generated without an energetic subaerial expression (as detected in the acoustic data). We term these events "silent VLPs." To our knowledge, these have only been reported in the literature during effusive activity at Stromboli in 2002 (Marchetti & Ripepe, 2005), 2007 (Ripepe et al., 2015) and 2014 (Ripepe et al., 2015, 2017). The lack of correspondence between VLPs and explosions during our study period is inconsistent with the "slug" model, which involves a gas bubble rising from some depth, expanding as pressure decreases, and then bursting at the lava free surface (Blackburn et al., 1976). Furthermore, previous work suggests silent VLPs during effusion have consistent characteristics with changing source depth (Marchetti & Ripepe, 2005; Ripepe et al., 2015, 2017) with an unchanged conduit geometry, and are therefore not related to a bubble interacting with a fixed structural feature in the subsurface such as a bend or flare in the conduit. We suggest the characteristics and timing of silent and non-silent VLPs and explosions are better explained by the plug model (Suckale et al., 2016), and attribute the VLP signal to the interaction between a rising gas slug and the base of a semi-rigid magma plug which inhibits rise to the vent and explosive gas release.

We suggest that the plug acts as a control on the mechanism of gas escape and effectively facilitates a diversity of surficial activity. The VLP is generated by a gas bubble impinging upon and moving into the plug. However,

10.1029/2022GL100735

the complex pathway structure in the plug controls the gas escape and causes it to be variable. Gas escape could be through pressurized, transient explosions (non-silent); jetting (non-silent); convective release of ash and gas (silent); or passive release (silent). These phenomena are all observed, often at the same time, at Stromboli (Harris & Ripepe, 2007). Analogue experiments examining gas bubble rise below and through a solid-rich suspension also support the plug model (Oppenheimer et al., 2020); results show that solids start to impact bubble flow at particle volume fraction of 30 vol% (45–60 vol% phenocrysts and microphenocrysts at Stromboli (Francalanci et al., 2004, 2005; Métrich et al., 2001). At particle fractions greater than 38 vol% rapidly expanding bubbles deformed and applied a high stress on the plug, but the bubbles were trapped when they were less overpressured. Silent VLPs may be generated by these less overpressured bubbles that can apply stress to the plug, but are ultimately trapped by it. Gas from these bubbles may escape through the plug, but at a rate that does not produce detectable audible or infrasonic signals. Conversely, VLPs with corresponding infrasonic signals of explosion are from bubbles with sufficient overpressure to ascend immediately through the plug and explode. The plug model allows for multiple bubbles rising in the conduit, which would allow for activity observed at Stromboli such as simultaneous explosions from different vents and continuous passive degassing with occasional explosions (Oppenheimer et al., 2020). Recent work suggests that Stromboli's activity is linked to near surface magma crystallinity and that variations in gas escape style are due to spatio-temporal variations in crystallinity or crystal-bubble interactions (Oppenheimer et al., 2020). The difference in gas ratios observed between passive and explosive degassing (Aiuppa et al., 2010; Burton et al., 2007) are compatible with the plug model. Gas bubbles from volatiles exsolving either from >4 km depth (CO_2-rich) or from <1 km depth could interact with the plug, generate a VLP, and pass through the plug as described previously. We note that the plug model of VLP dynamics offers a resolution to a long-standing conundrum in the relative timing of VLPs and associated explosions, which require unrealistically high gas ascent velocities to comply with the slug model (Harris & Ripepe, 2007; Ishii et al., 2019).

We observe two repeating VLP families with distinct dominant frequencies, 0.2 Hz (5 s) and 0.1 Hz (10 s) for F1 and F2 VLPs, respectively, but similar particle motions and depths. The different wavelengths suggest that two different scales of oscillation are excited. Perhaps the different length scales are due to the morphology of the bottom of the plug and how bubbles interact with it. We also observe that these VLPs occur with variable amplitudes, which suggests these oscillations can be excited with varying energy. It may be the variation in bubble size passing into the plug that determines amplitude. F1 VLPs occur at a higher rate relative to F2 VLPs. This may indicate a higher rate of gas and heat flow into the F1 pathway relative to F2 VLPs. Perhaps the F1 VLPs record the bubbles moving into the plug that feed the passively degassing, incandescent vent in the center of the crater. Additional observations, such as high-resolution gas imaging, may allow testing of this hypothesis.

6. "Slug" Versus "Plug" at Volcanoes Worldwide

We have addressed the high rate of repeating VLPs at Stromboli Volcano with little to no associated explosive gas escape and how these observations do not reconcile with the prevailing source (slug) model, but are well-explained by the plug model. Further analysis of the characteristics of these VLPs and inverting for their respective source mechanisms are critical next steps to understanding their source processes, particularly with respect to the plug model. The slug model has been invoked at a number of systems highlighted in Table 1 (e.g., Chouet et al., 2003; Knox et al., 2018; Kremers et al., 2013). Table 1 shows low-viscosity magma volcanoes with well-constrained crystallinity where VLPs have been observed during Strombolian activity and further analyzed for source characteristics documented in the literature. To our knowledge, these properties have only been documented for a small number of volcanoes despite the overall large number of geophysical and geochemical observations. This highlights the potential bias in our observations and understanding of VLPs in low-viscosity systems. Further, many volcano seismic deployments only consisted of short-period seismometers not sensitive to the VLP band. These limitations motivate future seismo-acoustic experiments to look for silent VLPs (notably those in bold as their vol% crystals is 38% or higher) and further investigate when the slug and plug models apply and improve understanding of their respective gas escape processes.

Table 1
Comparison of Very Long Period Seismic Events (VLPs) Observed at Volcanoes With Low Viscosity Magma

Volcano	Tectonic setting	wt% H_2O	Magma composition	VLP source depth [km]	vol% crystals
Erebus[a]	Intra	≤1.75 wt%	Phonolite	0.4	30%
Etna[b]	Sub	≤4 wt%	Basalt	0.83	30%–33%
Fuego [c]	Sub	≤6.2 wt%	Basaltic andesite	0.3	38%
Kilauea[d]	Intra	≤0.8 wt%	Basalt	1	16%
Stromboli [e]	Sub	≤3.8 wt%	Basalt	0.25	45%–60%
Yasur [f]	Sub	1 wt%	Basaltic andesite	1	35%–40%

[a](Aster et al., 2008; Knox et al., 2018; Moussallam et al., 2015). [b](Cannata et al., 2009; Métrich & Wallace, 2008; Spilliaert et al., 2006; Vona et al., 2011; Zuccarello et al., 2013). [c](Lyons & Waite, 2011; Oppenheimer et al., 2011; Rose et al., 2008; Waite et al., 2013; Walker et al., 2003). [d](Chevrel et al., 2018; Chouet et al., 2010; Wallace et al., 2015). [e](Chouet et al., 2003; Francalanci et al., 2004, 2005; Lautze & Houghton, 2007; Métrich et al., 2001; Métrich et al., 2010). [f](Barth et al., 2019; Kremers et al., 2013; Métrich et al., 2011).

7. Conclusion

During a period of low intensity, but normal, activity at Stromboli Volcano, we observed two families of repeating seismic VLPs. Using seismo-acoustic data we find that only about 4% of F1 VLPs and 28% of F2 VLPs have associated surficial explosions in the acoustic record. These two families of "silent VLPs" have roughly the same source location beneath the active crater based on particle motion analysis. We find the low occurrence of infrasound signals indicative of Strombolian explosions associated with VLPs does not support the prevailing gas slug VLP source model. We suggest the process of rising bubbles interacting with and passing into a complex, semi-permeable plug generates these silent VLPs and helps explain the variable acoustic and degassing regimes. At Stromboli, a natural next step for understanding the VLP characteristics and the processes at the base of the plug is through waveform source inversion; however, recent work shows this provides minimal constraints on the mechanism of Strombolian activity, and instead reflects conduit structure (Matoza et al., 2022). The infrasound signals (or lack there of) provide key support for the plug versus the slug model. Furthermore, the plug model of VLP dynamics offers a resolution to a long-standing conundrum in the relative timing of VLPs and associated explosions, which under the slug model require unrealistically high gas ascent velocities (Harris & Ripepe, 2007; Ishii et al., 2019; Patrick et al., 2011). Future integrated studies at other volcanoes are necessary to further understand shallow conduit processes and gas escape mechanisms and their respective seismo-acoustic signatures.

Data Availability Statement

The seismo-acoustic data used in the study are available through the IRIS DMC via https://doi.org/10.7914/SN/YI_2018. The PeakMatch software used for the multiplet analysis is available through GitHub at https://github.com/simonrodgers/peakmatch-xcorr (Rodgers et al., 2015). The wind data are from Visual Crossing available at https://www.visualcrossing.com/weather/weather-data-services.

Acknowledgments
K.F.M. thanks A. Aiuppa, M. Bitetto, S. Carn, V. Cigala, D. Delle Donne, H. Le Mevel, C. Sealing, and H. Tractorino for their help during the field campaign and S. Golden for his help in campaign preparations. Thank you to K. Cashman for thoughtful discussions. The authors thank Chris Huber for handling the manuscript as editor and Michael Heap, Nick Varley, Phillip Dawson, and three anonymous reviewers for their comments especially during the first year of the COVID-19 pandemic. The project was funded by NSF-PF-1725730. D.F. acknowledges support from NSF-EAR 190614.

References

Agostini, C., Fortunati, A., Arzilli, F., Landi, P., & Carroll, M. R. (2013). Kinetics of crystal evolution as a probe to magmatism at Stromboli (Aeolian Archipelago, Italy). *Geochimica et Cosmochimica Acta*, *110*, 135–151. https://doi.org/10.1016/j.gca.2013.02.027

Aiuppa, A., Bertagnini, A., Métrich, N., Moretti, R., Di Muro, A., Liuzzo, M., & Tamburello, G. (2010). A model of degassing for Stromboli volcano. *Earth and Planetary Science Letters*, *295*(1–2), 195–204. https://doi.org/10.1016/j.epsl.2010.03.040

Aster, R., Zandomeneghi, D., Mah, S., McNamara, S., Henderson, D. B., Knox, H., & Jones, K. (2008). Moment tensor inversion of very long period seismic signals from Strombolian eruptions of Erebus volcano. *Journal of Volcanology and Geothermal Research*, *177*(3), 635–647. https://doi.org/10.1016/j.jvolgeores.2008.08.013

Ballestracci, R. (1982). Self-potential survey near the craters of Stromboli volcano (Italy). Inference for internal structure and eruption mechanism. *Bulletin Volcanologique*, *45*(4), 349–365. https://doi.org/10.1007/BF02597257

Barth, A., Edmonds, M., & Woods, A. (2019). Valve-like dynamics of gas flow through a packed crystal mush and cyclic Strombolian explosions. *Scientific Reports*, *9*(1), 821. https://doi.org/10.1038/s41598-018-37013-8

Bertagnini, A., Métrich, N., Landi, P., & Rosi, M. (2003). Stromboli volcano (Aeolian Archipelago, Italy): An open window on the deep-feeding system of a steady state basaltic volcano. *Journal of Geophysical Research*, *108*(B7). https://doi.org/10.1029/2002jb002146

Blackburn, E. A., Wilson, L., & Sparks, R. S. (1976). Mechanisms and dynamics of Strombolian activity. *Journal of the Geological Society*, *132*(4), 429–440. https://doi.org/10.1144/gsjgs.132.4.0429

Blundy, J., Cashman, K., & Humphreys, M. (2006). Magma heating by decompression-driven crystallization beneath andesite volcanoes. *Nature*, *443*(7107), 76–80. https://doi.org/10.1038/nature05100

Bodurtha, F. T. (1980). *Industrial explosion prevention and protection* (1st ed.). McGraw-Hill.

Burton, M., Allard, P., Murè, F., & La Spina, A. (2007). Magmatic gas composition reveals the source depth of slug-driven Strombolian explosive activity. *Science*, *317*(5835), 227–230. https://doi.org/10.1126/science.1141900

Calvari, S., Spampinato, L., Lodato, L., Harris, A. J., Patrick, M. R., Dehn, J., et al. (2005). Chronology and complex volcanic processes during the 2002−2003 flank eruption at Stromboli volcano (Italy) reconstructed from direct observations and surveys with a handheld thermal camera. *Journal of Geophysical Research*, *110*(2), 1–23. https://doi.org/10.1029/2004JB003129

Cannata, A., Montalto, P., Privitera, E., & Russo, G. (2009). Characterization and location of infrasonic sources in active volcanoes: Mount Etna, September−November 2007. *Journal of Geophysical Research*, *114*(B8), B08308–B08315. https://doi.org/10.1029/2008JB006007

Chevrel, M. O., Harris, A. J., James, M. R., Calabrò, L., Gurioli, L., & Pinkerton, H. (2018). The viscosity of pāhoehoe lava: In situ syn-eruptive measurements from Kilauea, Hawaii. *Earth and Planetary Science Letters*, *493*, 161–171. https://doi.org/10.1016/j.epsl.2018.04.028

Chouet, B. A., Dawson, P., Ohminato, T., Martini, M., Saccorotti, G., Giudicepietro, F., et al. (2003). Source mechanisms of explosions at Stromboli volcano, Italy, determined from moment-tensor inversions of very-long-period data. *Journal of Geophysical Research*, *108*(B1), ESE7-1–ESE7-25. https://doi.org/10.1029/2002JB001919

Chouet, B. A., Dawson, P. B., James, M. R., & Lane, S. J. (2010). Seismic source mechanism of degassing bursts at Kilauea Volcano, Hawaii: Results from waveform inversion in the 10–50s band. *Journal of Geophysical Research*, *115*(9), 1–24. https://doi.org/10.1029/2009JB006661

Chouet, B. A., Saccorotti, G., Dawson, P., Martini, M., Scarpa, R., De Luca, G., et al. (1999). Broadband measurements of the sources of explosions at Stromboli volcano, Italy. *Geophysical Research Letters*, *26*(13), 1937–1940. https://doi.org/10.1029/1999GL900400

Conte, A. M., Perinelli, C., & Trigila, R. (2006). Cooling kinetics experiments on different Stromboli lavas: Effects on crystal morphologies and phases composition. *Journal of Volcanology and Geothermal Research*, *155*(3–4), 179–200. https://doi.org/10.1016/j.jvolgeores.2006.03.025

Falsaperla, S., Maiolino, V., Spampinato, S., Jaquet, O., & Neri, M. (2008). Sliding episodes during the 2002–2003 Stromboli lava effusion: Insights from seismic, volcanic, and statistical data analysis. *Geochemistry, Geophysics, Geosystems*, *9*(4). https://doi.org/10.1029/2007GC001859

Finizola, A., Sortino, F., Lénat, J. F., Aubert, M., Ripepe, M., & Valenza, M. (2003). The summit hydrothermal system of Stromboli. New insights from self-potential, temperature, CO_2 and fumarolic fluid measurements, with structural and monitoring implications. *Bulletin of Volcanology*, *65*(7), 486–504. https://doi.org/10.1007/s00445-003-0276-z

Francalanci, L., Davies, G. R., Lustenhouwer, W., Tommasini, S., Mason, P. R., & Conticelli, S. (2005). Intra-grain Sr isotope evidence for crystal recycling and multiple magma reservoirs in the recent activity of Stromboli volcano, Southern Italy. *Journal of Petrology*, *46*(10), 1997–2021. https://doi.org/10.1093/petrology/egi045

Francalanci, L., Tommasini, S., & Conticelli, S. (2004). The volcanic activity of Stromboli in the 1906–1998 AD period: Mineralogical, geochemical and isotope data relevant to the understanding of the plumbing system. *Journal of Volcanology and Geothermal Research*, *131*(1–2), 179–211. https://doi.org/10.1016/S0377-0273(03)00362-7

Genco, R., & Ripepe, M. (2010). Inflation-deflation cycles revealed by tilt and seismic records at Stromboli volcano. *Geophysical Research Letters*, *37*(12). https://doi.org/10.1029/2010GL042925

Harris, A., & Ripepe, M. (2007). Temperature and dynamics of degassing at Stromboli. *Journal of Geophysical Research*, *112*(3), 1–18. https://doi.org/10.1029/2006JB004393

Ishii, K., Yokoo, A., Kagiyama, T., Ohkura, T., Yoshikawa, S., & Inoue, H. (2019). Gas flow dynamics in the conduit of Strombolian explosions inferred from seismo-acoustic observations at Aso volcano, Japan. *Earth Planets and Space*, *71*(1), 1–15. https://doi.org/10.1186/s40623-019-0992-z

James, M. R., Lane, S. J., & Chouet, B. A. (2006). Gas slug ascent through changes in conduit diameter: Laboratory insights into a volcano-seismic source process in low-viscosity magmas. *Journal of Geophysical Research*, *111*(B5). https://doi.org/10.1029/2005JB003718

Kinney, G. F., & Graham, K. J. (1985). *Explosive shocks in air* (2nd ed.). Springer.

Kirchdörfer, M. (1999). Analysis and quasistatic FE modeling of long period impulsive events associated with explosions at Stromboli volcano (Italy). *Annals of Geophysics*, *42*(3), 1–12. https://doi.org/10.4401/ag-3728

Knox, H. A., Chaput, J. A., Aster, R. C., & Kyle, P. R. (2018). Multiyear shallow conduit changes observed with Lava Lake eruption seismograms at Erebus Volcano, Antarctica. *Journal of Geophysical Research: Solid Earth*, *123*(4), 3178–3196. https://doi.org/10.1002/2017JB015045

Kremers, S., Wassermann, J., Meier, K., Pelties, C., van Driel, M., Vasseur, J., & Hort, M. (2013). Inverting the source mechanism of Strombolian explosions at Mt. Yasur, Vanuatu, using a multi-parameter dataset. *Journal of Volcanology and Geothermal Research*, *262*, 104–122. https://doi.org/10.1016/j.jvolgeores.2013.06.007

Kundu, P. K., & Cohen, I. M. (2008). *Fluid mechanics* (4th ed.). Academic Press.

Lautze, N. C., & Houghton, B. F. (2007). Linking variable explosion style and magma textures during 2002 at Stromboli volcano, Italy. *Bulletin of Volcanology*, *69*(4), 445–460. https://doi.org/10.1007/s00445-006-0086-1

Lyons, J. J., & Waite, G. P. (2011). Dynamics of explosive volcanism at Fuego volcano imaged with very long period seismicity. *Journal of Geophysical Research*, *116*(B09303), 1–18. https://doi.org/10.1029/2011JB008521

Marchetti, E., & Ripepe, M. (2005). Stability of the seismic source during effusive and explosive activity at Stromboli volcano. *Geophysical Research Letters*, *32*(3), 1–5. https://doi.org/10.1029/2004GL021406

Marsella, M., Baldi, P., Coltelli, M., & Fabris, M. (2012). The morphological evolution of the Sciara del Fuoco since 1868: Reconstructing the effusive activity at Stromboli volcano. *Bulletin of Volcanology*, *74*(1), 231–248. https://doi.org/10.1007/s00445-011-0516-6

Matoza, R. S., Chouet, B. A., Jolly, A. D., Dawson, P. B., Fitzgerald, R. H., Kennedy, B. M., et al. (2022). High-rate very-long-period seismicity at Yasur Volcano, Vanuatu: Source mechanism and decoupling from surficial explosions and infrasound. *Geophysical Journal International*, *230*(1), 392–426. https://doi.org/10.1093/gji/ggab533

McKee, K., Roman, D. C., Fee, D., Ripepe, M., Aiuppa, A., & Waite, G. P. (2018). *Seismo-acoustic network at Stromboli volcano, Italy*. International Federation of Digital Seismograph Networks. https://doi.org/10.7914/SN/YI_2018

McKee, K., Roman, D. C., Fee, D., Waite, G. P., & Ripepe, M. (2019). Multiplet and particle motion analysis of very-long-period (VLP) events at Stromboli volcano, Italy, during a period of low surface activity in 2018. In *AGU fall meeting abstracts* (p. V44B–05). Retrieved from https://ui.adsabs.harvard.edu/abs/2019AGUFM.V44B.05M

Métrich, N., Allard, P., Aiuppa, A., Bani, P., Bertagnini, A., Shinohara, H., et al. (2011). Magma and volatile supply to post-collapse volcanism and block resurgence in Siwi caldera (Tanna Island, Vanuatu arc). *Journal of Petrology*, *52*(6), 1077–1105. https://doi.org/10.1093/petrology/egr019

Métrich, N., Bertagnini, A., & Di Muro, A. (2010). Conditions of magma storage, degassing and ascent at Stromboli: New insights into the volcano plumbing system with inferences on the eruptive dynamics. *Journal of Petrology*, *51*(3), 603–626. https://doi.org/10.1093/petrology/egp083

Métrich, N., Bertagnini, A., Landi, P., & Rosi, M. (2001). Crystallization driven by decompression and water loss at Stromboli volcano (Aeolian Islands, Italy). *Journal of Petrology*, *42*(8), 1471–1490. https://doi.org/10.1093/petrology/42.8.1471

Métrich, N., & Wallace, P. J. (2008). Volatile abundances in basaltic magmas and their degassing paths tracked by melt inclusions. *Reviews in Mineralogy and Geochemistry*, *69*(1), 363–402. https://doi.org/10.2138/rmg.2008.69.10

Moussallam, Y., Oppenheimer, C., Scaillet, B., Buisman, I., Kimball, C., Dunbar, N., et al. (2015). Megacrystals track magma convection between reservoir and surface. *Earth and Planetary Science Letters*, *413*, 1–12. https://doi.org/10.1016/j.epsl.2014.12.022

Neuberg, J., Luckett, R., Ripepe, M., & Braun, T. (1994). Highlights from a seismic broadband array on Stromboli volcano. *Geophysical Research Letters*, *21*(9), 749–752. https://doi.org/10.1029/94GL00377

Ohminato, T., Chouet, B. A., Dawson, P., & Kedar, S. (1998). Waveform inversion of very long period impulsive signals associated with magmatic injection beneath Kilauea Volcano, Hawaii. *Journal of Geophysical Research*, *103*(B10), 23839–23862. https://doi.org/10.1029/98JB01122

Oppenheimer, C., Moretti, R., Kyle, P. R., Eschenbacher, A., Lowenstern, J. B., Hervig, R. L., & Dunbar, N. W. (2011). Mantle to surface degassing of alkalic magmas at Erebus Volcano, Antarctica. *Earth and Planetary Science Letters*, *306*(3–4), 261–271. https://doi.org/10.1016/j.epsl.2011.04.005

Oppenheimer, J., Capponi, A., Cashman, K. V., Lane, S. J., Rust, A. C., & James, M. R. (2020). Analogue experiments on the rise of large bubbles through a solids-rich suspension: A "weak plug" model for Strombolian eruptions. *Earth and Planetary Science Letters*, *531*, 115931. https://doi.org/10.1016/j.epsl.2019.115931

Patrick, M., Wilson, D., Fee, D., Orr, T., & Swanson, D. (2011). Shallow degassing events as a trigger for very-long-period seismicity at Kīlauea Volcano, Hawai'i. *Bulletin of Volcanology*, *73*(9), 1179–1186. https://doi.org/10.1007/s00445-011-0475-y

Ripepe, M., Donne, D. D., Genco, R., Maggio, G., Pistolesi, M., Marchetti, E., et al. (2015). Volcano seismicity and ground deformation unveil the gravity-driven magma discharge dynamics of a volcanic eruption. *Nature Communications*, *6*(1), 1–6. https://doi.org/10.1038/ncomms7998

Ripepe, M., Donne, D. D., Harris, A., Marchetti, E., & Ulivieri, G. (2008). Dynamics of Strombolian activity. In S. Calvari, S. Inguaggiato, G. Puglisi, M. Ripepe, & M. Rosi (Eds.), *The Stromboli volcano: An integrated study of the 2002–2003 eruption* (pp. 39–48). AGU. https://doi.org/10.1029/182GM05

Ripepe, M., Marchetti, E., & Ulivieri, G. (2007). Infrasonic monitoring at Stromboli volcano during the 2003 effusive eruption: Insights on the explosive and degassing process of an open conduit system. *Journal of Geophysical Research*, *112*(B09207), B09207. https://doi.org/10.1029/2006JB004613

Ripepe, M., Marchetti, E., Ulivieri, G., Harris, A., Dehn, J., Burton, M., et al. (2005). Effusive to explosive transition during the 2003 eruption of Stromboli volcano. *Geology*, *33*(5), 341. https://doi.org/10.1130/G21173.1

Ripepe, M., Pistolesi, M., Coppola, D., Delle Donne, D., Genco, R., Lacanna, G., et al. (2017). Forecasting effusive dynamics and decompression rates by magmastatic model at open-vent Volcanoes. *Scientific Reports*, *7*(1), 3885. https://doi.org/10.1038/s41598-017-03833-3

Rodgers, M., Rodgers, S., & Roman, D. C. (2015). Peakmatch: A java program for multiplet analysis of large seismic datasets. *Seismological Research Letters*, *86*(4), 1208–1218. https://doi.org/10.1785/0220140160

Rose, W. I., Self, S., Murrow, P. J., Bonadonna, C., Durant, A. J., & Ernst, G. G. J. (2008). Nature and significance of small volume fall deposits at composite volcanoes: Insights from the October 14, 1974 Fuego eruption, Guatemala. *Bulletin of Volcanology*, *70*(9), 1043–1067. https://doi.org/10.1007/s00445-007-0187-5

Rowe, C. A., Aster, R. C., Kyle, P. R., Schlue, J. W., & Dibble, R. R. (1998). Broadband recording of Strombolian explosions and associated very-long-period seismic signals on Mount Erebus Volcano, Ross Island, Antarctica. *Geophysical Research Letters*, *25*(13), 2297–2300. https://doi.org/10.1029/98GL01622

Spilliaert, N., Allard, P., Métrich, N., & Sobolev, A. V. (2006). Melt inclusion record of the conditions of ascent, degassing, and extrusion of volatile-rich alkali basalt during the powerful 2002 flank eruption of Mount Etna (Italy). *Journal of Geophysical Research*, *111*(4), B04203. https://doi.org/10.1029/2005JB003934

Suckale, J., Keller, T., Cashman, K. V., & Persson, P.-O. (2016). Flow-to-fracture transition in a volcanic mush plug may govern normal eruptions at Stromboli. *Geophysical Research Letters*, *43*(23), 12071–12081. https://doi.org/10.1002/2016GL071501

Taddeucci, J., Edmonds, M., Houghton, B., James, M. R., & Vergniolle, S. (2015). Hawaiian and Strombolian eruptions. In *The Encyclopedia of Volcanoes* (2nd. ed., pp. 485–503). Elsevier. https://doi.org/10.1016/B978-0-12-385938-9.00027-4

Tam, C. K. (1998). Jet noise: Since 1952. *Theoretical and Computational Fluid Dynamics*, *10*(1–4), 393–405. https://doi.org/10.1007/s001620050072

Thorarinsson, S., Steinthórsson, S., Einarsson, T., Kristmannsdóttir, H., & Oskarsson, N. (1973). The eruption on Heimaey, Iceland. *Nature*, *241*(5389), 372–375. https://doi.org/10.1038/241372a0

Vona, A., Romano, C., Dingwell, D. B., & Giordano, D. (2011). The rheology of crystal-bearing basaltic magmas from Stromboli and Etna. *Geochimica et Cosmochimica Acta*, *75*(11), 3214–3236. https://doi.org/10.1016/j.gca.2011.03.031

Waite, G. P., Nadeau, P. A., & Lyons, J. J. (2013). Variability in eruption style and associated very long period events at Fuego Volcano, Guatemala. *Journal of Geophysical Research: Solid Earth*, *118*(4), 1526–1533. https://doi.org/10.1002/jgrb.50075

Walker, J. A., Roggensack, K., Patino, L. C., Cameron, B. I., & Matías, O. (2003). The water and trace element contents of melt inclusions across an active subduction zone. *Contributions to Mineralogy and Petrology*, *146*(1), 62–77. https://doi.org/10.1007/s00410-003-0482-x

Wallace, P. J., Plank, T., Edmonds, M., & Hauri, E. H. (2015). Chapter 7—Volatiles in magmas. In *The Encyclopedia of Volcanoes* (pp. 163–183). Elsevier.

Wielandt, E., & Forbriger, T. (1999). Near-field seismic displacement and tilt associated with the explosive activity of Stromboli. *Annali di Geofisica*, *42*(3), 407–416. https://doi.org/10.4401/ag-3723

Zuccarello, L., Burton, M. R., Saccorotti, G., Bean, C. J., & Patanè, D. (2013). The coupling between very long period seismic events, volcanic tremor, and degassing rates at Mount Etna volcano. *Journal of Geophysical Research: Solid Earth*, *118*(9), 4910–4921. https://doi.org/10.1002/jgrb.50363